LIMNOLOGY and OCEANOGRAPHY

Elemental and macromolecular composition of the marine Chloropicophyceae, a major group of oceanic photosynthetic picoeukaryotes

Vinitha Ebenezer [1]*, Yingyu Hu [1], Olga Carnicer [2], Andrew J. Irwin [3], Michael J. Follows [3], Zoe V. Finkel [1]

[1]Department of Oceanography, Dalhousie University, Halifax, Nova Scotia, Canada
[2]Department of Mathematics and Statistics, Dalhousie University, Halifax, Nova Scotia, Canada
[3]Department of Earth, Atmospheric and Planetary Science, Massachusetts Institute of Technology, Cambridge, Massachusetts

Abstract

Chloropicophyceae (Prasinophyte Clade VII) are small nonmotile coccoid cells with cell diameters ranging from 1 to 3 μm. Molecular surveys indicate they are relatively high in abundance in moderately oligotrophic oceanic waters and may substantively contribute to biogeochemical cycling in the sea. Here, we quantify the elemental and macromolecular composition of three subtropical Chloropicophyceae strains: *Chloropicon mariensis*, *Chloropicon maureeniae*, and *Chloropicon roscoffensis* under nutrient-sufficient exponential growth and nitrate starvation. Under nutrient-sufficient conditions the Chloropicophyceae are high in C : N and quite low in C : P and N : P relative to the canonical Redfield ratio, reflecting their relatively high nucleic acid composition compared to many other phytoplankton taxa. Nitrate starvation causes increases in C : N and C : P and decreases in N : P, primarily due to increases in carbohydrate and lipid and decreases in protein and RNA. There is genetic evidence that unlike most other green algae, Chloropicophyceae are diploid. The high nucleic acid content in the *Chloropicon* is consistent with the hypothesis that the nucleus, as a nonscalable component, takes up a larger and substantial proportion of cell mass in diploid picoeukaryotes. The elemental and macromolecular composition of these Chloropicophyceae, and relatively homeostatic response to N-starvation compared to diatoms, provides some insight into their success in the moderately oligotrophic ocean.

Photosynthetic picoeukaryotes, characterized by a cell diameter between 0.2 and 3 μm, are common in the sea surface (Worden and Not 2008; Freitas et al. 2020) and often contribute substantively to primary productivity in moderately oligotrophic regions (Not et al. 2004; Lepére et al. 2009; Massana et al. 2011). Chlorophyta are common constituents of marine photosynthetic picoeukaryotes communities (Simmons et al. 2016; Tragin and Vaulot 2019). *Micromonas*, *Bathycoccus*, and *Ostreococcus*, class Mamiellophyceae, tend to be most abundant in the coastal regions (Not et al. 2004; Karlusich et al. 2020), although they can also be found in open ocean regions (Joli et al. 2017;

Leconte et al. 2020). By contrast, the relatively newly described class Chloropicophyceae (Prasinophyte Clade VII) tend to be the more dominant Chlorophyta in moderately oligotrphic waters (Lopes dos Santos et al. 2016, 2017a,b; Karlusich et al. 2020). Based on metabarcode data from the *Tara* expedition, the Chlorophyta sequences constitute an average of 16–20% of the photosynthetic sequences in the sea surface and deep chlorophyll maximum in the 0.8–5 μm size fraction (Lopes dos Santos et al. 2017a; Carradec et al. 2018). The Chloropicophyceae represent a majority of the Chlorophyta sequences in these samples, up to a maximum of 99.9% (Lopes dos Santos et al. 2017a).

Chloropicophyceae are nonmotile coccoid cells, mostly 1.5–3 μm in diameter, have a single nucleus, mitochondria, and chloroplast with a starch grain, and a suite of carotenoids that includes violaxanthin, lutein, astaxanthin or antheraxanthin, but lack prasinoxanthin which is present in several other small marine green phytoplankton taxa including *Ostreococcus* (Lopes dos Santos et al. 2017a). The Chloropicophyceae have been divided into 10 clades (A1–A7, B1–B3) and two genera: *Chloropicon* (Clade A) and *Chloroparvula* (Clade B) (Lopes dos Santos et al. 2017b). Few morphological or ultrastructural

*Correspondence: vebenezer@dal.ca

features differentiate *Chloropicon* from *Chloroparvula* although *Chloropicon* species are more likely to have a fibrous vs. smooth cell wall, a larger starch grain, and granules within the cytoplasm (Lopes dos Santos et al. 2017*b*). The specific niches of the Chloropicophyceae clades are not yet well characterized, but they have been found in latitudes ranging from 34°S to 60°N (Lopes dos Santos et al. 2017*b*; Vorobev et al. 2020).

A characterization of the physiology, macromolecular, and elemental composition of the Chloropicophyceae is needed to improve our understanding of their contribution to the marine food web and elemental cycling (Galbraith and Martiny 2017; Inomura et al. 2020). At present, we have some physiological, elemental, and biochemical data on key Mamiellophyceae taxa (Halsey et al. 2014; Garcia et al. 2018; Liefer et al. 2019), but there is comparatively less information on the Chloropicophyceae. Lopes dos Santos et al. (2017*b*) in their description of the Class characterized their ultrastructure, pigment content, and DNA content. Lemieux et al. (2019) determined that *Chloropicon primus* differs in several key genes and pathways from the Mamiellophyceae, and unlike the Mamiellophyceae and most other unicellular green algae, *C. primus* is diploid. Here, we quantify the C : N : P and macromolecular composition of three subtropical strains of Chloropicophyceae under exponential nonlimiting conditions and nitrogen starvation conditions to better understand the impact of their small size and diploidy on their macromolecular and elemental composition. We hypothesize that diploidy and very small size constrains Chloropicophyceae to be high in DNA, and therefore cellular phosphorus, relative to similar sized haploids such as the Mamiellophyceae or larger eukaryotic phytoplankton such as diatoms (Raven 1994; Raven et al. 2005). Furthermore, we hypothesize that a C-rich wall and high surface area to volume may result in relatively high C : N relative to larger eukaryotic phytoplankton, especially as compared to diatoms with their Si-based wall (Raven 1994; Finkel et al. 2016). Finally, we hypothesize that due to both their small size and adaptation to moderately oligotrophic regimes (Lopes dos Santos et al. 2017*b*), open-ocean Chloropicophyceae may exhibit less change in their elemental and macromolecular composition in response to nitrogen starvation than coastal Mamiellophyceae and rapidly growing diatom taxa (Garcia et al. 2018; Liefer et al. 2019).

Materials and methods
Species and culture conditions

The species studied here, *Chloropicon mariensis* (strain RCC138, clade A2), *Chloropicon maureeniae* (strain RCC3374, clade A7), and *Chloropicon roscoffensis* (strain RCC3375, clade A5), were obtained from the Roscoff Culture Collection (RCC). The three species are pelagic and were isolated from the oligotrophic Pacific Ocean (22.75°N, 158.00°W, Station ALOHA). All the strains were maintained under an irradiance of 100 μmol photons m^{-2} s^{-1} with a 12 h : 12 h light : dark

cycle, temperature of 22°C, pH of 8.1, and a salinity of 32. The cultures were grown in the media used to maintain the strains in the culture collection (RCC). *C. maureeniae* was grown in K media (Keller et al. 1987) in an enriched artificial seawater water base (ESAW) following Berges et al. (2001) with sodium nitrate (882 μM) and ammonium chloride (50 μM) used as the N source and disodium β-glycerophosphate (14.2 μM) used as the P source. *C. mariensis* and *C. roscoffensis* were grown in f/2 (Guillard and Ryther 1962) with an ESAW base with sodium nitrate (882 μM) used as the N source and sodium dihydrogen phosphate (36 μM) as the P source. Cultures were maintained in exponential growth in semicontinuous batch cultures in 5-L glass bottles containing 4.5 L of media. The cultures were manually shaken gently twice a day, as the cultures responded negatively to vigorous mixing. Cultures were maintained in triplicate, kept optically thin (between a minimum cell density of 50, 000 cells mL^{-1} and a maximum cell density of 1,400,000 cells mL^{-1}), in exponential growth phase, in nutrient-replete conditions for a minimum of 10 generations to acclimate them to their conditions before sampling and the initiation of the nitrogen starvation treatment as well as to determine their resource-replete growth rate. Preliminary batch experiments were conducted to determine the range of cell densities required to keep the cultures in exponential, resource-replete conditions for the nutrient-replete component of the experiment. The pH of the medium was monitored with a VWR sympHony benchtop meter.

Cell volume estimation

Samples for cell volume were collected from each replicate bottle in replete exponential growth and over the nutrient starvation treatment. Immediately after sampling, cells were preserved in Lugol's solution at room temperature, and after 3–4 h, images of a minimum of 100 cells were taken at ×100 magnification using a Zeiss Axioimager A1 (Zeiss, Oberkochen, Germany). Cell diameter was measured from the images, calibrated with a Zeiss micrometer, using ImageJ (Schneider et al. 2012). Cell volume was calculated assuming the cells were spheres.

Cell counts and growth rate

Samples to monitor the cell density of *Chloropicon* and bacteria in the cultures were taken from each bottle replicate, on each harvesting day. Samples were preserved with 1% formaldehyde and then stored at −20°C until analyses. Before analysis the samples were thawed and 10% SYBR Green-I was added to 1 mL of the sample (to help detect the bacteria) and incubated at room temperature in the dark for 15 min. The cell densities of the phytoplankton and contaminating bacteria were measured with a BD Accuri C6 flow cytometer as described by Marie et al. (2005), with 3-μm fluorescence beads (Fluoresbrite Fluorescent Microspheres) used as an internal standard. A subset of *Chloropicon* cell density estimates were compared to counts made using a hemocytometer and light microscope (ZEISS Axioimager A1) at ×40 magnification; the

difference in cell density estimates was less than 20% between the methods. The exponential growth rate was monitored from the changes in cell density over the 10 generations prior to the initiation of the nitrate starvation treatment, and varied over time by less than 10%.

The nitrogen starvation treatment

Acclimated nutrient-replete cultures in triplicate bottles were sampled and then diluted to 50,000 cell mL^{-1} into media (as described above for each of the species) with no nitrogen added (Supporting Information Fig. S1). A small amount of residual nitrogen was transferred with the cells into the N-starvation treatment, but dissolved nitrogen in the media was monitored and was undetectable by Day 9 of the starvation treatment (Supporting Information Fig. S2). Samples were collected daily for cell counts and the decline in growth rate (μ) was estimated from the daily change in cell density (Supporting Information Fig. S2). Samples were collected by gentle filtration (2.45 psi) from each replicate bottle the first day of the treatment (Day 0) and then 7, 9, 12, and 15 d into nitrate starvation for: particulate elemental analysis including carbon (C), nitrogen (N), total particulate phosphorus (TPP), and intracellular phosphorus (IP); macromolecular analyses including bulk protein, carbohydrate, lipid, and phosphorus associated with the lipid fraction, RNA, DNA, chlorophyll *a* (Chl *a*), and polyphosphate; and the filtrate was taken from these samples to monitor inorganic nitrogen and phosphorus concentration in the media. A set of preliminary experiments established that precombusted (4 h at 450°C) GF/F filters and 0.6-μm pore sized 47-mm Whatman Nucleopore polycarbonate membrane filters provided similar, high harvesting efficiencies for Chloropicophyceae cells and minimized the number of bacteria captured on the filters (Supporting Information Fig. S3). Samples for elemental analysis (C, N, and P), carbohydrate, lipid, Chl *a*, and polyphosphate were collected on precombusted GF/F filters. To differentiate between intracellular and extracellular phosphorus two samples were taken, one rinsed with unenriched ESAW and the other with an oxalate reagent (Tovar-Sanchez et al. 2003) to remove surface adsorbed P. Samples for protein, RNA, and DNA were collected on 0.6-μm pore sized 47-mm Whatman Nucleopore polycarbonate membrane filters. Samples for elemental analysis, Chl *a*, and polyphosphate were stored immediately at −20°C. Samples for macromolecular analyses were immediately placed in liquid nitrogen and then stored at −80°C until analysis. Prior to analysis, all the samples were freeze-dried overnight (FreeZone 2.5 L −50°C Benchtop Freeze Dryers, LABCONCO). Dissolved nutrient samples were stored in the freezer at −20°C until analysis.

Dissolved nutrient and particulate elemental analyses

Dissolved nitrate and phosphate was monitored throughout the N-starvation treatment from the culture media filtered through GF/F precombusted filters. Nitrate was analyzed using a 42iQ NO–NO$_2$–NO*x* Analyzer (Thermo Scientific). Phosphate was measured using a SEAL AutoAnalyzer 3 HR following the phosphomolybdate method specified by the manufacturer. For particulate carbon and nitrogen analyses, culture biomass and blanks on precombusted GF/F filters were dried at 60°C for 2 d, pelleted in pressed tin capsules, and analyzed with a UNICUBE Vario MICRO cube elemental analyzer. Precision on %N and %C is 0.5%. For TPP and IP analyses, samples on precombusted GF/F filters were dried with 2 mL 0.017 M MgSO$_4$, combusted at 500°C for 6 h and then digested by 0.2 M HCl at 90°C for 30 min (Solorzano and Sharp 1980). Phosphorus was quantified using an ammonium molybdate method (Chen et al. 1956), modified for a microplate reader (Varioskan LUX multimode) (Liefer et al.

Macromolecular analyses

Extraction and analysis for protein follows methods described in Ni et al. (2017). In brief, protein samples on polycarbonate filters (0.6 μm) were extracted by bead milling (FastPrep Lysing Matrix D) in 1× protein extraction buffer (lithium dodecyl sulfate, pefabloc, and Tris). Bead milling was performed four times for 1 min at 6.5 ms^{-1}, with samples placed on ice for 2 min between each round of bead milling to prevent degradation by heating. Extracted protein was then quantified using the BioRad DC Assay and microplate reader (Varioskan LUX). Bovine gamma globulin was used as a standard. Carbohydrate samples on precombusted GF/F filters were hydrolyzed in H$_2$SO$_4$ (1 M) at 100°C for 1.5 h for *C. mariensis* and *C. maureeniae* and 2 h for *C. roscoffensis*. The extracted carbohydrate was measured with phenol sulfuric acid following Dubois et al. (1956), using a microplate reader. Glucose was used as the standard. Lipid samples on GF/F were extracted and purified using a modified Folch et al. method (Folch et al. 1957; Liefer et al. 2019). Prior to the addition of the Folch reagent (2:1 chloroform-methanol v/v), 100 μl water of Millipore water (Liefer et al. 2019) was added, the samples were rapidly frozen and rethawed twice before the addition of 2 mL of the solvent, vortexed (VWR Analog Vortex Mixer), and then sonicated using a sonication bath. To enhance extraction, the procedure was repeated four times and the extracts were pooled. The extract was filtered to remove non-lipid substances. KCl of 0.88% was added to the filtrate to form a biphasic system. The lower phase with extracted lipids was collected and dried under N$_2$ gas flow. The acid-dichromate method was used to quantify the extracted lipid (Pande et al. 1963). Next, 500 μL of 0.15% acid-dichromate was added to the dried sample. Glyceryl tripalmitate was used as the standard. The absorbance was read at 348 nm (Hu and Finkel 2020b). DNA and RNA were extracted from samples on polycarbonate filters by bead milling (FastPrep Lysing Matrix D) using an extraction buffer that included 0.5% *n*-lauryl sarcosine, 5 mM Tris, and 1 mM EDTA four times for 30 s at 6.5 m s^{-1}, with samples placed on ice for 2 min between each round of bead milling. The homogenate was centrifuged

(Eppendorf Centrifuge 5424 R) at 12,000 rpm for 5 min, the supernatant vortexed (VWR Analog Vortex Mixer) for 60 min at room temperature. Aliquots of extracts for each sample were treated with RNase, DNase, and RNase + DNase, and stained with SYBR Green II. RNA and DNA were then determined by SYBR Green II fluorescence, with corrections applied based on the background fluorescence present after nuclease treatment. RNA was quantified against an *Escherichia coli* ribosomal RNA standard (Ambion #7940) and DNA was quantified against a Type IX calf thymus DNA standard (Sigma# D4522). RNA and DNA fluorescence were determined in a 96-well opaque black microplate. The nucleic acid estimation method used is a modified version of Berdalet et al. (2005). Intracellular polyphosphate (poly-P) was estimated using a modified version of the 4′,6-diamidino-2-phenylindole (DAPI) method described by Aschar-Sobbi et al. (2008) and Martin and Van Mooy (2013), as described in Hu and Finkel (2020a). Tris buffer was added to freeze-dried samples on pre-combusted GF/F filters, sonicated, and kept in a boiling water bath for 15 min. This extraction process was repeated 8–10 times, the extracts were pooled and centrifuged (Eppendorf Centrifuge 5424 R) at 12,000 rpm for 5 min, then DAPI was added and poly-P quantified using an opaque black microplate and microplate reader. A lid with a black film is used to avoid photobleaching DAPI-stained samples and then removed before the microplate measurement. Analytical grade sodium polyphosphate (poly-P) was used as a standard.

Data analysis

The percentage of carbon, nitrogen, and phosphorus contributed by macromolecules were computed from the elemental composition of biochemical classes compiled by Geider and LaRoche (2002), Sterner and Elser (2002) for RNA and DNA, and Jeffrey et al. (1997) for Chl *a*. Elemental and macromolecular ratios under replete conditions were scaled by the average ratio across all three *Chloropicon* spp. (reported as "Scaled ratio") to facilitate comparisons to two species of diatoms and two species of Mamiellophyceae from a study that used the same methods to determine elemental and macromolecular composition (Liefer et al. 2019). We also computed the elemental and macromolecular ratios after 12 d of N starvation relative to the observed ratios under replete conditions (reported as "N starved/replete"). To compare elemental ratios across *Chloropicon* spp., we performed an ANOVA on the log ratios followed by a Tukey Honest Significant Difference test to perform pair-wise *t*-tests. Means and confidence intervals for all ratios were computed on the log ratios but transformed back to their natural scale for reporting. All data analyses were performed using the statistical software R version 4.0.3. Error estimates provided in figures, results and the discussion are one standard deviation, unless otherwise noted.
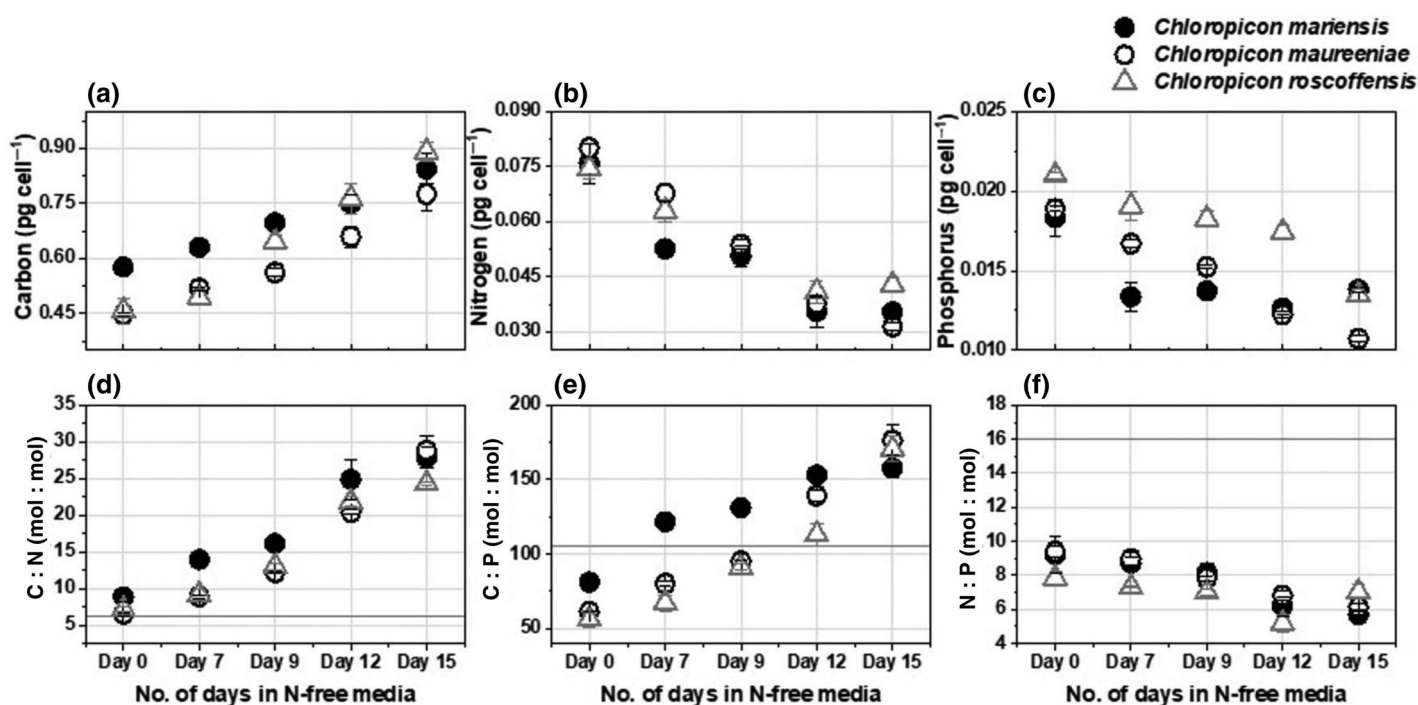
Results

Growth rate, C, N, P composition, and cell volume under resource-replete and N-starvation conditions

The data for all replicates are deposited at figshare.org (Ebenezer et al. 2021).

Cellular C, N, and P contents were measured under resource-replete exponential growth (Day 0) and over several days of increasing nitrogen starvation (Days 7, 9, 12, and 15) (Fig. 1). The acclimated exponential resource-replete growth rate of the three *Chloropicon* species examined here ranged from 0.65 ± 0.01 d^{-1} (*C. mariensis*), 0.61 ± 0.01 d^{-1} (*C. maureeniae*), to 0.76 ± 0.03 d^{-1} (*C. roscoffensis*). The decline in growth rate over the nitrogen starvation treatment was estimated from the daily change in cell density over the nitrogen starvation treatment. By Day 7 in the N-starvation treatment growth rate had declined $39.3\% \pm 1.6\%$ for *C. mariensis*, $38.6\% \pm 2.3\%$ for *C. maureeniae*, and $14.2\% \pm 4.1\%$ for *C. roscoffensis* relative to the exponential resource-replete conditions. Although some dissolved inorganic nitrogen (DIN) was transferred with culture at the beginning of the N-starvation treatment (Supporting Information Fig. S2), DIN was below detection while phosphate was in excess of 6 μM by Day 7 of the N-starvation treatment (Supporting Information Fig. S2). Between Days 12 and 15 of the treatment, DIN was undetectable and growth rate was negative, reflecting a decrease in cell density over this time period. Bacterial density and pH increases become more pronounced at Day 12 (Supporting Information Fig. S2). We therefore focus much of our analyses and discussion on Day 0 (N-replete) and Day 12 of the N-starvation treatment, in particular because as bacterial densities increase they could begin to contribute to the particulate biomass (Supporting Information Fig. S2). Based on the bacterial densities (Supporting Information Figs. S2, S3) and assuming marine bacteria are approximately 13.86 fg C cell^{-1} and 2.6 fg N cell^{-1}, 0.7 fg P cell^{-1} on our filters (Fagerbakke et al. 1996; Fukuda et al. 1998), we estimate that bacteria biomass contributed < 1% C (across species), < 1% N, and < 1% P on Day 12 of the experiment.

All the *Chloropicon* species exhibited a decrease in cellular N content, more moderate decreases in intracellular P content, and increases in cellular C content with increasing N-starvation (Fig. 1). By Day 12 of N-starvation, cellular N content decreased by between 45% and 53%, intracellular P decreased between 17% and 35%, and cellular C increased between 23% and 40%, across the three species. Note TPP decreased between 19% and 37%, across the species with N-starvation (Supporting Information Fig. S4).

Under N-replete exponential growth conditions, the three species of Chloropicophyceae have a mean C : N : P of 64.5 : 8.7 : 1; note that P refers to intracellular phosphorus (Fig. 1; Supporting Information Table S1). The C : N : P of *C. mariensis*, *C. maureeniae*, and *C. roscoffensis* is 78.2 : 8.8 : 1, 62.2 : 9.4 : 1, and 56.1 : 7.8 : 1, respectively. After 12 d of N-starvation, the three Chloropicophyceae species have a mean

Fig. 1. C, N, P content and ratios under resource replete exponential growth conditions (Day 0) and N-starvation conditions. Error bars represent 1 SD on $N = 3$. (**a**) Cellular carbon content (pg cell^{-1}), (**b**) cellular nitrogen content (pg cell^{-1}), (**c**) IP content (pg cell^{-1}), (**d**) C : N (mol : mol), (**e**) C : P (mol : mol), and (**f**) N : P (mol : mol). The gray line is the Redfield ratio. Each species is represented by a different symbol: *Chloropicon mariensis* as black circles, *Chloropicon maureeniae* as open black circles, *Chloropicon roscoffensis* as open gray triangles.

C : N : P of 140:6.3:1 (Supporting Information Table S1). The C : N : P of *C. mariensis*, *C. maureeniae*, and *C. roscoffensis* is 153 : 6.2 : 1, 139 : 6.8 : 1 and, 128 : 5.8 : 1, respectively. Across the species under resource-replete conditions, C : N and C : P were significantly higher in *C. mariensis* relative to *C. roscoffensis*, and N : P was higher in *C. maurenniae* than in *C. roscoffensis*. After 12 d of N-starvation, only C : P significantly varied across the species (Supporting Information Table S1).
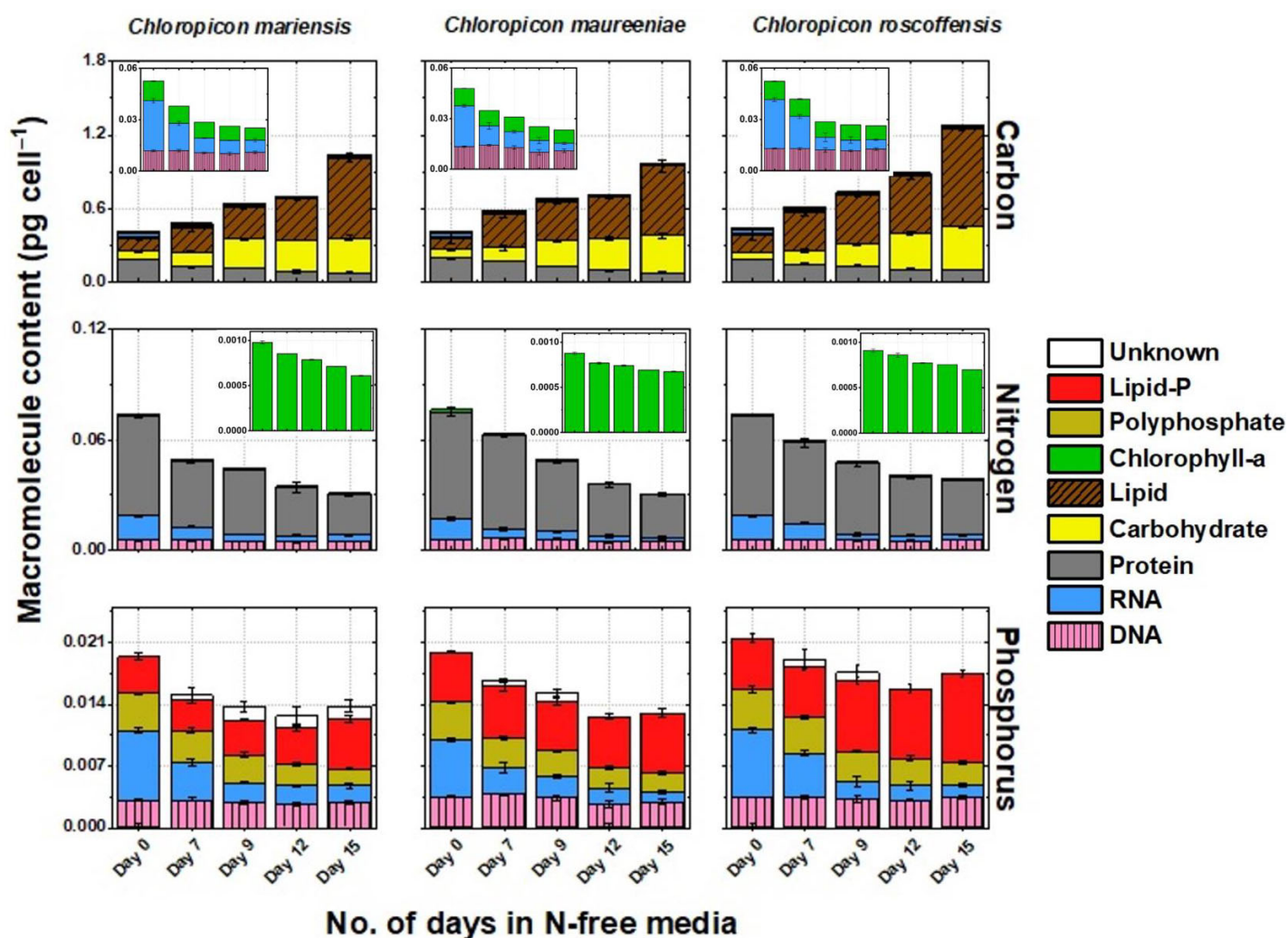
Despite the increases in cellular C content between N-replete conditions and after 12 d of N-starvation, cell volume modestly declined in all the species. Average cell volume across the strains ranges from 1.67 ± 0.3 to $1.44 \pm 0.11\ \mu m^3$ for *C. maureeniae*, between 1.98 ± 0.32 and $1.87 \pm 0.28\ \mu m^3$ for *C. mariensis*, and between $2.90 \pm 0.28\ \mu m^3$ and $2.11 \pm 0.05\ \mu m^3$ for *C. roscoffensis* under N-replete conditions (Day 0) and after 12 d of N-starvation, respectively (Supporting Information Table S2).

Macromolecular composition and contribution to cellular C, N, and P

In the Chloropicophyceae, much of cellular carbon is in protein (31–43%, range refers to the means across the three species examined under resource-replete exponential growth), followed by lipid (18–32%), and then carbohydrate (12–15%); most of cellular nitrogen is in protein (71–72%) with much smaller but substantive allocations to RNA (13–17%) and DNA (7.0–7.7%); the largest macromolecular pool contributing to intracellular P is RNA (36–42%), followed by polyphosphate stores (21–23%), and

then DNA (16–17%) (Fig. 2). Phospholipid contributed between 21% and 60% and uncharacterized phosphorus pools contributed less than 10% to IP content, respectively. In some cases macromolecular P accounts for more than 100% of IP (Fig. 1 and 2). IP (TPP − adsorbed P) content was between ~ 80% and 90% of TPP, depending on the strain, and varied little with N-starvation (Supporting Information Fig. S4). Chl *a* accounts for between 1.9% and 2.3% of cellular C and cellular N.

Nitrogen starvation in the Chloropicophyceae causes carbohydrate and lipid content to increase, protein, RNA, Chl *a*, and polyphosphate content to decrease, and no change in DNA content (Fig. 2; Supporting Information Fig. S5; Table S3). There is little change in phospholipid content with N-starvation in *C. mariensis* and *C. maureeniae* but there is a small increase in *C. roscoffensis*. The decreases in phospholipid and polyphosphate content are much smaller than the changes in RNA and chlorophyll (Fig. 2; Supporting Information Fig. S5; Table S3). After 12 d of N-starvation, protein accounts a much smaller fraction of cellular carbon (11–14%) while lipid and carbohydrate account for much larger fractions (44–61% and 34–38%, respectively) relative to under resource-replete growth conditions (Fig. 2). Chl *a*, DNA, and RNA account for 1.1–1.3% (range is mean across species), 1.3–1.5%, and 0.8–1.1% of cellular carbon after 12 d of N-starvation. Cellular nitrogen allocation after 12 d of N-starvation is 70–72% protein, 11.0–12.9% DNA, 7–10% RNA, 1.8–2% Chl *a*. P allocation was 9–16% RNA, 17–21% DNA, and 17–18% polyphosphate and 6.6–10.2% phospholipid.
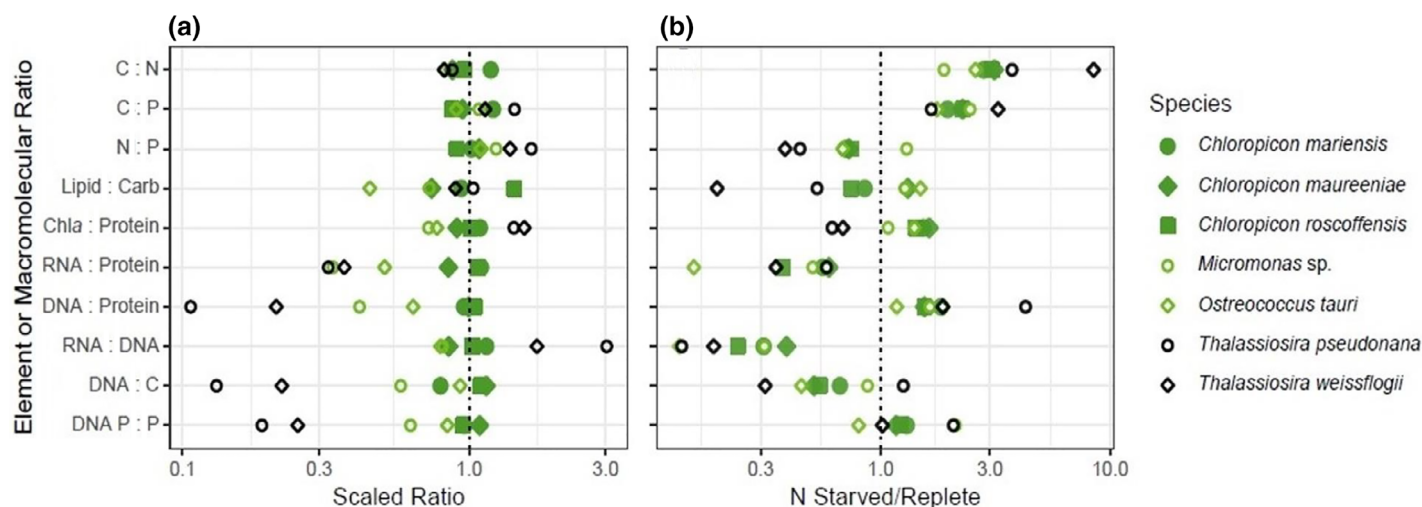
Fig. 2. Carbon, nitrogen, and IP content (pg cell^{-1}) allocated to macromolecules. Data shown are the average of three replicates for each species. Inset figures highlight macromolecules with small contribution to total C or N.

We compared the elemental and macromolecular ratios of the Chloropicophyceae examined in this study to two Mamiellophyceae species: *Ostreococcus tauri* and *Micromonas* sp. and two diatom species: *Thalassiosira pseudonana* and *Thalassiosira weissflogii* that were examined using a similar experimental design in a previous study (Liefer et al. 2019). The Chloropicophyceae examined are much higher in DNA : C, DNA : protein, and RNA : protein and lower in Chl *a* : protein than diatoms under resource-replete, exponential growth conditions (Fig. 3a). This comparison indicates that the Chloropicophyceae are higher in nucleic acid content than these other eukaryotes, and more of the their total cellular phosphorus is in DNA (DNA P : P). In general, the Chlorophytes, both the Chloropicophyceae and Mamiellophyceae exhibit less change in their elemental and macromolecular ratios after 12 d of N-starvation than the diatoms (N-starved/replete conditions, Fig. 3b).

In aggregate, the major macromolecules measured here account for in excess of 97% of the total particulate carbon, 91% of the particulate nitrogen, and 56% of the IP measured. Note that under resource-replete conditions, RNA, DNA, polyphosphate, and phospholipids accounts for between 80% and 88% (across species) of intracellular P, but under N-starved conditions this drops to approximately 70% for *C. maureeniae* and *C. roscoffensis* and to 57% for *C. mariensis* (Supporting Information Table S4). ATP may account for some of the intracellular P (Holm-Hansen 1973).

Discussion

Chlorophytes are among the most numerically dominant groups contributing to marine photosynthetic eukaryote communities in the less than 3-μm size class (Simmons et al. 2016; Tragin and Vaulot 2019). In coastal regions, *Ostreococcus*,

Fig. 3. Comparison of dimensionless elemental molar ratios and macromolecular mass ratios across species under resource-replete conditions (**a**) and under N-starvation compared to replete conditions (**b**). Ratios in the left panel (**a**) are scaled to the *Chloropicon* spp. average to facilitate cross-species comparisons across ratios. All ratios are reported on a log axis to transform multiplicative effects into distances and to enable comparison across large ranges. The vertical dashed line highlights the *Chloropicon* spp. average (**a**) and replete conditions (**b**). Data on the diatoms: *Thalassiosira pseudonana*, *T. weissflogii*, and Mamiellophyceae: *Ostreococcus tauri*, and *Micromonas* sp. are from Liefer et al. (2019). DNA P : P is the fraction of total cellular P in DNA.

Micromonas, and *Bathycoccus*, members of the class Mamiellophyceae, are often dominant contributors to photosynthetic picoeukaryote communities (Not et al. 2004; Karlusich et al. 2020), while in more oceanic regions, *Chloropicon* and *Chloroparvula* of the class Chloropicophyceae are more likely to be dominant constituents of photosynthetic picoeukaryotes communities (Lopes dos Santos et al. 2017*a*,b; Turmel et al. 2019). While there is some work on the physiology and elemental composition of Mamiellophyceae (Garcia et al. 2018; Liefer et al. 2019), data on the growth rate, elemental (C : N : P), and macromolecular composition of the Chloropicophyceae is lacking. Here, we characterize the elemental and macromolecular composition of three *Chloropicon* species under resource-replete exponential growth and under nitrogen-starvation conditions to aid in our understanding of their niche and influence on food web quality and the biogeochemical cycles of C, N, and P.

The average molar C : N : P of subtropical Pacific *C. mariensis*, *C. maureeniae*, and *C. roscoffensis* under resource-replete conditions is 65 : 8.7 : 1 (Fig. 1; Supporting Information Table S1). This is high in C : N (7.5), and much lower in C : P and N : P, than the traditional Redfield ratio for marine planktonic particulate material of 106C : 16N : 1P (Redfield 1934), the updated global particulate organic material estimate of 146C : 20N : 1P (Martiny et al. 2013) and the average ratio (132C : 18N : 1P) reported by Quigg et al. (2011) for 29 phytoplankton species grown under laboratory conditions. The C : P and N : P of the Chloropicophyceae are similar to the values reported for other photosynthetic picoeukaryotes grown under resource-replete conditions, including

Micromonas sp. and *Ostreococcus* sp. (Garcia et al. 2018; Liefer et al. 2019; Supporting Information Table S2). In contrast, the N : P of the marine picocyanobacteria *Prochlorococcus* and *Synechococcus* ranges between 21 and 33 under resource-replete conditions (Bertilsson et al. 2003). The relatively high C : N in the Chloropicophyceae is consistent with a C-rich cell wall (Lopes dos Santos et al. 2017*b*) and their high surface area to volume ratio due to their small cell volume (Finkel et al. 2010; Finkel et al. 2016), while their relatively low C : P and N : P largely reflects their relatively high nucleic acid content relative to protein content (Figs. 2, 3) in addition to their phosphorus stores (Raven 2013; Martin et al. 2014). There are statistically significant differences in the C : N : P across the three species examined: *C. mariensis* is generally higher in carbon (Fig. 3) and *C. roscoffensis* is higher in phosphorus (Fig. 3), but these differences are small relative to the increases in C : N and C : P and decreases in N : P associated with N-starvation (Fig. 1; Supporting Information Table S1). These three species represent the A2, A7, and A5 Chloropicophyceae clades (Lopes dos Santos et al. 2017*b*) and their species-level biochemical differences may reflect their distinct evolutionary histories and niches (Lopes dos Santos et al. 2017*b*).

The environmental preferences and biogeography of marine Chloropicophyceae and their constituent clades are not yet well characterized but they appear to dominate photosynthetic picoeukaryote communities under moderately oligotrophic conditions (Lopes dos Santos et al. 2017*b*; Lemieux et al. 2019; Vorobev et al. 2020). Allometric perspectives (Irwin et al. 2006; Finkel et al. 2010) would suggest that they would be outcompeted by smaller picocyanobacteria, such as

Prochlorococcus and *Synechoccocus* spp., under extremely oligotrophic conditions (Ward et al. 2012). To better understand how the Chloropicophyceae respond to nutrient regimes we evaluated their elemental and macromolecular composition in response to nitrogen starvation. Qualitatively the Chloropicophyceae respond to N-starvation in a manner similar to many other microalgae previously examined (Finkel et al. 2016; Liefer et al. 2019): growth rate slows and then arrests, protein and RNA content declines while carbohydrate and lipid accumulates (Fig. 2; Supporting Information Fig. S4). Because protein is especially N rich, RNA is particularly P rich, and carbohydrate and lipid are C rich, after 12 d of N-starvation the average C : N : P of the Chloropicophyceae shifts to 140 : 6.3 : 1 (Figs. 1, 2; Supporting Information Table S1). The change in C : N : P by the Chloropicophyceae in response to nitrogen starvation is much smaller than what has been observed for diatoms, but similar to what has been observed for other Chlorophytes (Liefer et al. 2019), in particular *Micromonas* and *Ostreococcus* (Fig. 3; Supporting Information - Table S2). In response to N-starvation, the marine Chlorophyte picoeukaryotes increase more in lipid than carbohydrates than diatoms (Fig. 3); this may be because stored lipid (triacylglycerides [TAG]) takes up less physical space per unit C (Raven 1986; Finkel et al. 2016; Liefer et al. 2019). This biochemical strategy may support the competitive ability of these eukaryotes, relative to TAG-poor picocyanobacteria, under some energy and/or nutrient-limited regimes (Becker et al. 2018).

While small cell size confers a large number of advantages for unicellular marine photoautotrophs such as high surface area to volume ratio and nutrient diffusion rates and low sinking rates out of the sunlit surface (Raven 1994; Finkel et al. 2010), extremely small size imposes constraints that can impact the elemental and macromolecular composition and physiological capabilities of photosynthetic eukaryotes. In a series of papers, Raven (1986, 1994, 1998) demonstrated that DNA and membranes are nonscalable components, meaning they constitute an increasing fraction of total cellular biomass below a minimum cell size, and as a consequence limit the minimum viable size of photoautotrophs and influence both the growth rates and the macromolecular and elemental composition of small picoeukaryotes. For example, Raven (1994) calculated that the molar C : N : P of a 0.5 μm diameter Chlorophyte, without a C-rich cell wall, would be 64 : 11 : 1, based on nonscalable components. No data were available at the time to test this hypothesis. Our estimate of *Chloropicon* spp. C : N : P is similar to this estimate. *Chloropicon* is 1.5–3 μm in diameter and has a C-rich wall (Lopes dos Santos et al. 2017*b*), likely accounting for its higher C : N content than the estimates provided by Raven (1986, 1994, 1998). The lower than predicted N : P of the *Chloropicon* under resource-replete conditions reflects their high nucleic acid content for a cell of their size: the *Chloropicon* species examined here are significantly higher in DNA : protein than *Micromonas* and an

approximate order of magnitude higher than the diatom *T. pseudonana* (see Fig. 3). This raises the question—Why are the Chloropicophyceae so high in DNA?

Ostreococcus is the smallest known photosynthetic eukaryotic cell, ~ 1 μm in diameter (Courties et al. 1998), and has the smallest known green algal genome (Courties et al. 1998; Derelle et al. 2006; Lemieux et al. 2019): the genome of *Ostreococcus lucimarinus* is 13.2 Mb (Palenik et al. 2007) and *O. tauri* is 12.5 Mb (Derelle et al. 2006). *Bathycoccus* and *Micromonas* are slightly larger cells and have slightly larger genomes: *Bathycoccus prasinos* is 15.0 Mb (Moreau et al. 2012), *Micromonas commoda* is 21.0 Mb (Worden et al. 2009), and *M. pusilla* is 22.0 Mb (Worden et al. 2009). Lopes dos Santos et al. (2017*b*) examined 45 Chloropicophyceae species with average cell diameters ranging from 1.5 to 3 μm and found DNA content ranges from 20 to 70 Mb (DNA was quantified using a flow cytometric method). Although most green microalgae are haploid in their vegetative growth stage (Otto and Gerstein 2008), Lemieux et al. (2019) recently determined that *C. primus* (RCC 15/CCMP 1205) is diploid (with one trisomic chromosome), with a genome size of 17.4 Mb. The genome of *C. primus* is relatively compressed and has several genes/pathways not found in Mamiellophyceae, including thiamine synthesis and a more complete set of genes for branched chain amino acid catabolism (Lemieux et al. 2019). The *Chloropicon* spp. examined in this study have an average DNA content ranging from 0.033 to 0.037 pg cell^{-1}. If the Chloropicophyceae examined here are haploid, their genome size would range between 32.2 and 36.2 Mb, but if diploid then their average genome sizes range from 16.1 to 18.1 Mb (following Doležel et al. 2003). At present, it is not definitively known if these species of marine Chloropicophyceae are haploid or diploid, but if they are haploid they would have very anomalously large genomes relative to similarly sized marine Chlorophyta. A number of hypotheses have been advanced regarding the relative advantages and disadvantages for a haploid vs. a diploid life cycle (Lewis Jr 1985; Otto and Gerstein 2008). Haploids will have lower resource requirements (especially for P) and lower energetic costs associated with synthesizing their DNA, while diploids may have an increased buffer against genetic load and have enhanced genetic complexity to respond to a wider range of biotic and environmental challenges (Suda and Watanabe 1989; Otto and Gerstein 2008). Moreover, diploidy might help cells withstand partial genome degradation due to viral infection (Zborowskya and Lindell 2019). Here, we find DNA accounts for 17–19% of the Chloropicophyceae IP content, slightly higher than for the haploid Mamiellophyceae (12–15%), but much higher than for the much larger diploid diatoms (4%) (Fig. 3). We anticipate that diploidy has a range of consequences for macromolecular content and growth rate of the Chloropicophyceae species relative to Mamiellophyceae species such as *Ostreococcus*. Diploid Chloropicophyceae are higher in DNA content relative similarly sized haploid species

(Fig. 3). This higher DNA content influences their N and P allocation budget, reducing the amount of these resources available for other processes, including growth rate. Raven (1994) hypothesized and provided some limited evidence that smaller Chlorophyte picoeukaryotes would have lower growth rates because they had to allocate a much larger proportions of their mass to membranes and DNA than larger cells. The maximum growth rate of the three *Chloropicon* species examined in this study is between 0.6 and 0.7 d^{-1}, considerably slower than maximum growth rates of many larger Chlorophyte species with cell volumes in the range of 10–100 μm^3 (see Raven 1994).

The *Chloropicon* spp. also have a very high ratio of RNA to protein compared to other eukaryotic phytoplankton taxa (Fig. 3). While the RNA to protein ratio is greatly elevated, the RNA to DNA ratio is only slightly larger in the Chloropicophyceae compared to Mamiellophyceae taxa. We speculate that the differences in these ratios across these groups are a result of resource allocation constraints imposed by the combination of diploidy and nonscalable components. Compared to the haploid Mamiellophyceae, the *Chloropicon* examined here devote more N and P to nucleic acids and thus have less protein per cell for other structural and functional activities. While higher RNA content and RNA : protein ratios are often linked to higher growth rate (Nicklisch and Steinberg 2009) here we propose that the high RNA : protein in the (potentially diploid) Chloropicophyceae reflects, in part, their high DNA content and maintenance of a reasonable ratio of RNA relative to DNA content. Their RNA : DNA is low compared to diatoms, but similar to other Chlorophytes (Fig. 3). In aggregate this evidence indicates that the maximum growth rate of the Chloropicophyceae may be limited by the availability of protein (Raven 1994) and this may reduce their competitive ability in variable and nutrient-rich environments, while the advantages of diploidy, their unique set of genes (Lemieux et al. 2019), and their relatively small size compared to other photosynthetic eukaryotes, may be critical factors for their success in moderately oligotrophic regions. We hypothesize the allocation strategies exhibited by the Chloropicophyceae species reflect an intermediate approach to many trade-offs: small, but not the smallest in physical size; slow-growing, but not the slowest; and acclimated to moderately oligotrophic but not the most oligotrophic waters. In aggregate, these results support the hypothesis that the Chloropicophyceae have a suite of physiological and biochemical strategies that optimize their competitive ability under moderately oligotrophic and moderately variable environments relative to diatoms. They are generally well adapted to respond to more variable and higher nutrient conditions compared to the very small picocyanobacteria that are so well adapted to very stable and very low-nutrient conditions. These hypotheses should be tested by expanding our data on the biogeography and ploidy (de Vries et al. 2021) of marine photosynthetic picoeukaryotes as well as their C, N, and P allocation to macromolecules under a range of environmental conditions.

References

Aschar-Sobbi, R., A. Y. Abramov, C. Diao, M. E. Kargacin, G. J. Kargacin, R. J. French, and E. Pavlov. 2008. High sensitivity, quantitative measurements of polyphosphate using a new DAPI-based approach. J. Fluoresc. **18**: 859–866. doi:10.1007/s10895-008-0315-4

Becker, K. W., and others. 2018. Daily changes in phytoplankton lipidomes reveal mechanisms of energy storage in the open ocean. Nat. Commun. **9**: 5179. doi:10.1038/s41467-018-07346-z

Berdalet, E., C. Roldán, M. P. Olivar, and K. Lysnes. 2005. Quantifying RNA and DNA in planktonic organisms with SYBR Green II and nucleases. Part A. Optimisation of the assay. Sci. Mar. **69**: 1–16. doi:10.3989/SCIMAR.2005.69N11

Berges, J. A., D. J. Franklin, and P. J. Harrison. 2001. Evolution of an artificial seawater medium: Improvements in enriched seawater, artificial water over the last two decades. J. Phycol. **37**: 1138–1145. doi:10.1046/j.1529-8817.2001.01052.x

Bertilsson, S., O. Berglund, D. Karl, and S. W. Chisholm. 2003. Elemental composition of marine *Prochlorococcus* and *Synechococcus*: Implications for the ecological stoichiometry of the sea. Limnol. Oceanogr. **48**: 1721–1731. doi:10.4319/lo.2003.48.5.1721

Carradec, Q., and others. 2018. A global ocean atlas of eukaryotic genes. Nat. Commun. **9**: 373. doi:10.1038/s41467-017-02342-1

Chen, P., T. T. Toribara, and H. Warner. 1956. Microdetermination of phosphorus. Anal. Chem. **28**: 1756–1758. doi:10.1021/ac60119a033

Courties, C., R. Perasso, M.-J. Chrétiennot-Dinet, M. Gouy, L. Guillou, and M. Troussellier. 1998. Phylogenetic analysis and genome size of *Ostreococcus tauri* (Chlorophyta, Prasinophyceae). J. Phycol. **34**: 844–849. doi:10.1046/j.1529-8817.1998.340844.x

de Vries, J., F. Monteiro, G. Wheeler, A. Poulton, J. Godrijan, F. Cerino, E. Malinverno, G. Langer, and C. Brownlee. 2021. Haplo-diplontic life cycle expands coccolithophore niche. B.G. **18**: 1161–1184. doi:10.5194/bg-18-1161-2021

Derelle, E., and others. 2006. Genome analysis of the smallest free-living eukaryote *Ostreococcus tauri* unveils many unique features. Proc. Natl. Acad. Sci. USA **103**: 11647–11652. doi:10.1073/pnas.0604795103

Doležel, J., J. Bartoš, H. Voglmayr, and J. Greilhuber. 2003. Nuclear DNA content and genome size of trout and human. Cytom. A **51A**: 127–128. doi:10.1002/cyto.a.10013

DuBois M., Gilles K. A., Hamilton J. K., Rebers P. A., Smith F. 1956. Colorimetric method for determination of sugars and related substances. Anal. Chem. **28**: 350–356. doi:10.1021/ac60111a017

Ebenezer, V., Y. Y. Hu, O. Carnicer, A. J. Irwin, M. J. Follows & Z. V. Finkel 2021. Elemental and macromolecular composition of three species of Chloropicophyceae. Dataset deposited at Figshare.com. doi:10.6084/m9.figshare.14749524

Fagerbakke, K. M., M. Heldal, and S. Norland. 1996. Content of carbon, nitrogen, oxygen, sulfur and phosphorus in native aquatic and cultured bacteria. Aquat. Microb. Ecol. **10**: 15–27. doi:10.3354/ame010015

Finkel, Z. V., J. Beardall, K. J. Flynn, A. Quigg, T. A. V. Rees, and J. A. Raven. 2010. Phytoplankton in a changing world: Cell size and elemental stoichiometry. J. Plankton Res. **32**: 119–137. doi:10.1093/plankt/fbp098

Finkel, Z. V., M. J. Follows, J. D. Liefer, C. M. Brown, I. Benner, and A. J. Irwin. 2016. Phylogenetic diversity in the macromolecular composition of microalgae. PLoS One **11**: e0155977. doi:10.1371/journal.pone.0155977

Folch, J., M. Lees, and S. G. Stanley. 1957. A simple method for the isolation and purification of total lipids from animal tissues. J. Biol. Chem. **226**: 497–509. doi:10.1083/jcb.1.2.173

Freitas, F. H., M. Dugenne, F. Ribalet, A. Hynes, B. Barone, D. Karl, and A. White. 2020. Diel variability of bulk optical properties associated with the growth and division of small phytoplankton in the North Pacific Subtropical Gyre. Appl. Optics **59**: 6702–6716. doi:10.1364/AO.394123

Fukuda, R., H. Ogawa, T. Nagata, and I. Koike. 1998. Direct determination of carbon and nitrogen contents of natural bacterial assemblages in marine environments. Appl. Environ. Microbiol. **64**: 3352–3358. doi:10.1128/AEM.64.9.3352-3358.1998

Galbraith, E. D., and A. C. Martiny. 2017. A simple nutrient-dependence mechanism for predicting the stoichiometry of marine ecosystems. Proc. Natl. Acad. Sci. USA **112**: 8199–8204. doi:10.1073/pnas.1423917112

Garcia, N. S., J. Sexton, T. Riggins, J. Brown, M. W. Lomas, and A. C. Martiny. 2018. High variability in cellular stoichiometry of carbon, nitrogen, and phosphorus within classes of marine eukaryotic phytoplankton under sufficient nutrient conditions. Front. Microbiol. **9**: 543. doi:10.3389/fmicb.2018.00543

Geider, R. J., and J. LaRoche. 2002. Redfield revisited: Variability of C:N:P in marine microalgae and its biochemical basis. Eur. J. Phycol. **37**: 1–17. doi:10.1017/S0967026201003456

Guillard, R. R. L., and J. H. Ryther. 1962. Studies of marine planktonic diatoms. I. *Cyclotella nana* Hustedt and *Detonula confervacea* (Cleve) Gran. Can. J. Microbiol. **8**: 229–239. doi:10.1139/m62-029

Halsey, K. H., A. J. Milligan, and M. J. Behrenfeld. 2014. Contrasting strategies of photosynthetic energy utilization drive lifestyle strategies in ecologically important picoeukaryotes. Metabolites **4**: 260–280. doi:10.3390/metabo4020260

Holm-Hansen, O. 1973. The use of ATP determinations in ecological studies. Bull. Ecol. Commun. **17**: 215–222.

Hu, Y. Y. and Z. V. Finkel 2020a. Inorganic polyphosphate in microalgae: A DAPI-based quantification in microtiter plate. doi:10.17504/protocols.io.b3xkqpkw

Hu, Y. Y. and Z. V. Finkel 2020b. Lipids in microalgae: Quantitation by acid-dichromate method in microtiter plate. doi:10.17504/protocols.io.bamiic4e

Inomura, K., A. W. Omta, D. Talmy, J. Bragg, C. Deutsch, and M. J. Follows. 2020. A mechanistic model of macromolecular allocation, elemental stoichiometry, and growth rate in phytoplankton. Front. Microbiol. **11**: 86. doi:10.3389/fmicb.2020.00086

Irwin, A. J., Z. V. Finkel, O. Schofield, and P. G. Falkowski. 2006. Scaling-up from nutrient physiology to the size-structure of phytoplankton communities. J. Plankton Res. **28**: 459–471. doi:10.1093/plankt/fbi148

Jeffrey, S. W., R. F. C. Mantoura, and T. Bjørnland. 1997. Data for the identification of 47 key phytoplankton pigments, p. 449–559. *In* S. W. Jeffrey, R. F. C. Mantoura, and S. W. Wright [eds.], Phytoplankton pigments in oceanography: Guidelines to modern methods. Monographs on oceanographic methodology. UNESCO.

Joli, N., A. Monier, R. Logares, and C. Lovejoy. 2017. Seasonal patterns in Arctic prasinophytes and inferred ecology of *Bathycoccus* unveiled in an Arctic winter metagenome. ISME J. **11**: 1372–1385. doi:10.1038/ismej.2017.7

Karlusich, J. J. P., F. M. Ibarbalz, and C. Bowler. 2020. Phytoplankton in the Tara Ocean. Ann. Rev. Mar. Sci. **12**: 233–265. doi:10.1146/annurev-marine-010419-010706

Keller, M. D., R. C. Selvin, W. Claus, and R. R. L. Guillard. 1987. Media for the culture of oceanic ultraphytoplankton. J. Phycol. **23**: 633–638. doi:10.1111/j.1529-8817.1987.tb04217.x

Leconte, J., L. F. Benites, T. Vannier, P. Wincker, G. Piganeau, and O. Jaillon. 2020. Genome resolved biogeography of Mamiellales. Genes **11**: 66. doi:10.3390/genes11010066

Lemieux, C., M. Turmel, C. Otis, and J.-F. Pombert. 2019. A streamlined and predominantly diploid genome in the tiny marine green alga *Chloropicon primus*. Nat. Commun. **10**: 4061. doi:10.1038/s41467-019-12014-x

Lepére, C., D. Vaulot, and D. J. Scanlan. 2009. Photosynthetic picoeukaryote community structure in the South East Pacific Ocean encompassing the most oligotrophic waters on Earth. Environ. Microbiol. **11**: 3105–3117. doi:10.1111/j.1462-2920.2009.02015.x

Lewis, W. M., Jr. 1985. Nutrient scarcity as an evolutionary cause of haploidy. Am. Nat. **125**: 692–701. doi:10.1086/284372

Liefer, J. D., A. Garg, M. H. Fyfe, A. J. Irwin, I. Benner, C. M. Brown, M. J. Follows, A. W. Omta, and Z. V. Finkel. 2019. The macromolecular basis of phytoplankton C: N: P under nitrogen starvation. Front. Microbiol. **10**: 763. doi:10.3389/fmicb.2019.00763

Lopes dos Santos, A., P. Gourvil, F. Rodriguez-Hernandez, J. L. Garrido, and D. Vaulot. 2016. Photosynthetic pigments of oceanic Chlorophyta belonging to prasinophytes clade VII. J. Phycol. **52**: 148–155. doi:10.1111/jpy.12376

Lopes dos Santos, A., P. Gourvil, M. Tragin, M.-H. Noël, J. Decelle, S. Romac, and D. Vaulot. 2017a. Diversity and oceanic distribution of Prasinophytes clade VII, the dominant group of green algae in oceanic waters. ISME J. **11**: 512–528. doi:10.1038/ismej.2016.120

Lopes dos Santos, A., and others. 2017b. Chloropicophyceae, a new class of picophytoplanktonic prasinophytes. Sci. Rep. **7**: 14019. doi:10.1038/s41598-017-12412-5

Marie, D., N. Simon, and D. Vaulot. 2005. Phytoplankton cell counting by flow cytometry, p. 253–267. *In* R. A. Andersen [ed.], Algal culturing techniques. Elsevier. doi:10.1016/B978-012088426-1/50018-4

Martin, P., and B. A. S. Van Mooy. 2013. Fluorometric quantification of polyphosphate in environmental plankton samples: Extraction protocols, matrix effects, and nucleic acid interference. Appl. Environ. Microbiol. **79**: 273–281. doi:10.1128/AEM.02592-12

Martin, P., S. T. Dyhrman, M. W. Lomas, N. J. Poulton, and B. A. S. Van Mooy. 2014. Accumulation and enhanced cycling of polyphosphate by Sargasso Sea plankton in response to low phosphorus. Proc. Natl. Acad. Sci. USA **111**: 8089–8094. doi:10.1073/pnas.1321719111

Martiny, A. C., C. T. A. Pham, F. W. Primeau, J. A. Vrugt, K. J. Moore, and others. 2013. Strong latitudinal patterns in the elemental ratios of marine plankton and organic matter. Nat. Geosci. **6**: 279–283. doi:10.1038/ngeo1757,

Massana, R., M. Pernice, J. A. Bunge, and J. D. Campo. 2011. Sequence diversity and novelty of natural assemblages of picoeukaryotes from the Indian Ocean. ISME J. **5**: 184–195. doi:10.1038/ismej.2010.104

Moreau, H., and others. 2012. Gene functionalities and genome structure in *Bathycoccus prasinos* reflect cellular specializations at the base of the green lineage. Genome Biol. **13**: R74. doi:10.1186/gb-2012-13-8-r74

Ni, G., G. Zimbalatti, C. D. Murphy, A. B. Barnett, C. M. Arsenault, G. Li, A. M. Cockshutt, and D. A. Campbell. 2017. Arctic *Micromonas* uses protein pools and non-photochemical quenching to cope with temperature restrictions on Photosystem II protein turnover. Photosynth. Res. **131**: 203–220. doi:10.1007/s11120-016-0310-6

Nicklisch, A., and C. E. W. Steinberg. 2009. RNA/protein and RNA/DNA ratios determined by flow cytometry and their relationship to growth limitation of selected planktonic algae in culture. Eur. J. Phycol. **44**: 297–308. doi:10.1080/09670260802578518

Not, F., M. Latasa, D. Marie, T. Cariou, D. Vaulot, and N. Simon. 2004. A single species, *Micromonas pusilla* (Prasinophyceae), dominates the eukaryotic picoplankton in the western English Channel. Appl. Environ. Microbiol. **70**: 4064–4072. doi:10.1128/AEM.70.7.4064-4072.2004

Otto, S. P., and A. C. Gerstein. 2008. The evolution of haploidy and diploidy. Curr. Biol. **18**: R1121–R1124. doi:10.1016/j.cub.2008.09.039

Palenik, B., J. Grimwood, A. Aerts, and others. 2007. The tiny eukaryote *Ostreococcus* provides genomic insights into the paradox of plankton speciation. Proc. Natl. Acad. Sci. USA **104**: 7705–7710. doi:10.1073/pnas.0611046104,

Pande, S. V., P. Khan, and T. A. Venkitasubramanian. 1963. Microdetermination of lipids and serum total fatty acids. Anal. Biochem. **6**: 415–423. doi:10.1016/0003-2697(63)90094-0

Quigg, A., A. J. Irwin, and Z. V. Finkel. 2011. Evolutionary inheritance of elemental stoichiometry in phytoplankton. Proc. R. Soc. B **278**: 526–534. doi:10.1098/rspb.20.010.1356

Raven, J. A. 1986. Physiological consequences of extremely small size for autotrophic organisms on the sea. Can. J. Fish. Aquat. Sci. **214**: 1–70.

Raven, J. A. 1994. Why are there no picoplanktonic O_2 evolvers with volumes less than 10^{-19} m^3? J. Plankton Res. **16**: 565–580. doi:10.1093/plankt/16.5.565

Raven, J. A. 1998. The twelfth Tansley lecture. Small is beautiful: The picophytoplankton. Funct. Ecol. **12**: 503–513. doi:10.1046/j.1365-2435.1998.00233.x

Raven, J. A. 2013. RNA function and phosphorus use by photosynthetic organisms. Front. Plant Sci. **4**: 536. doi:10.3389/fpls.2013.00536

Raven, J. A., Z. V. Finkel, and A. J. Irwin. 2005. Picophytoplankton: Bottom-up and top-down controls on ecology and evolution. Vie Et Milieu **55**: 209–215.

Redfield, A. C. 1934. On the proportions of organic derivations in sea water and their relation to the composition of plankton, p. 177–192. *In* R. J. Daniel [ed.], James Johnstone memorial volume. Univ. Press of Liverpool.

Schneider, C. A., W. S. Rasband, and K. W. Eliceiri. 2012. NIH image to ImageJ: 25 years of image analysis. Nat. Methods **9**: 671–675. doi:10.1038/nmeth.2089

Simmons, M. P., S. Sudek, A. Monier, A. J. Limardo, V. Jimenez, C. R. Perle, V. A. Elrod, J. T. Pennington, and A. Z. Worden. 2016. Abundance and biogeography of picoprasinophyte ecotypes and other phytoplankton in the Eastern North Pacific Ocean. Appl. Environ. Microbiol. **82**: 1693–1705. doi:10.1128/AEM.02730-15

Solorzano, L., and J. H. Sharp. 1980. Determination of total dissolved phosphorus and particulate phosphorus in natural waters. Limnol. Oceanogr. **25**: 754–758. doi:10.4319/lo.1980.25.4.0754

Sterner, R. W., and J. J. Elser. 2002. Ecological stoichiometry: The biology of elements from molecules to the biosphere. Princeton Univ. Press. Available at https://www.jstor.org/stable/j.ctt1jktrp3.

Suda, S., and M. M. Watanabe. 1989. Evidence for sexual reproduction in the priminitive green alga *Nephroselmis olivaceae* (Prasinophyceae). J. Phycol. **25**: 596–600. doi:10.1111/j.1529-8817.1989.tb00266.x

Tovar-Sanchez, A., S. A. Sañudo-Wilhelmya, M. Garcia-Vargas, R. S. Weaver, L. C. Popels, and D. A. Hutchins. 2003. A

trace metal clean reagent to remove surface-bound iron from marine phytoplankton. Mar. Chem. **82**: 91–99. doi: 10.1016/S0304-4203(03)00054-9

Tragin, M., and D. Vaulot. 2019. Novel diversity within marine Mamiellophyceae (Chlorophyta) unveiled by metabarcoding. Sci. Rep. **9**: 5190. doi:10.1038/s41598-019-41680-6

Turmel, M., A. Lopes dos Santos, C. Otis, R. Sergerie, and C. Lemieux. 2019. Tracing the evolution of the plastome and mitogenome in the Chloropicophyceae uncovered convergent tRNA gene losses and a variant plastid genetic code. Genome Biol. Evol. **11**: 1275–1292. doi:10.1093/gbe/evz074

Vorobev, A., M. Dupouy, Q. Carradec, T. Delmont, A. Annamalé, P. Wincker, and E. Pelletier. 2020. Transcriptome reconstruction and functional analysis of eukaryotic marine plankton communities via high-throughput metagenomics and metatranscriptomics. Genome Res. **30**: 647–659. doi:10.1101/gr.253070.119

Ward, B. A., S. Dutkiewicz, O. Jahn, and M. J. Follows. 2012. A size-structured food-web model for the global ocean. Limnol. Oceanogr. **57**: 1877–1891. doi:10.4319/lo.2012.57.6.1877

Worden, A. Z., and F. Not. 2008. Ecology and diversity of picoeukaryotes, p. 159–205. *In* D. L. Kirchman [ed.], Microbial ecology of the oceans, 2nd ed. John Wiley & Sons. doi: https://doi.org/10.1002/9780470281840.ch6

Worden, A. Z., and others. 2009. Green evolution and dynamic adaptations revealed by genomes of the marine picoeukaryotes *Micromonas*. Science **324**: 268–272. doi:10.1126/science.1167222

Zborowskya, S., and D. Lindell. 2019. Resistance in marine cyanobacteria differs against specialist and generalist cyanophages. Proc. Natl. Acad. Sci. USA **116**: 16899–16908. doi:10.1073/pnas.1906897116

Acknowledgments

Conflict of interest

None declared.